

Investigation of phase matching for third-harmonic generation in silicon slow light photonic crystal waveguides using Fourier optics

Christelle Monat,^{1,*} Christian Grillet,¹ Bill Corcoran,¹ David J. Moss,¹
Benjamin J. Eggleton,¹ Thomas P. White,² and Thomas F. Krauss²

¹ Institute of Photonics and Optical Science (IPOS), Centre for Ultrahigh-bandwidth Devices for Optical Systems (CUDOS), School of Physics, The University of Sydney, NSW 2006, Australia

² School of Physics and Astronomy, University of St Andrews, St Andrews, Fife, KY16 9SS, UK
*monat@physics.usyd.edu.au

Abstract: Using Fourier optics, we retrieve the wavevector dependence of the third-harmonic (green) light generated in a slow light silicon photonic crystal waveguide. We show that quasi-phase matching between the third-harmonic signal and the fundamental mode is provided in this geometry by coupling to the continuum of radiation modes above the light line. This process sustains third-harmonic generation with a relatively high efficiency and a substantial bandwidth limited only by the slow light window of the fundamental mode. The results give us insights into the physics of this nonlinear process in the presence of strong absorption and dispersion at visible wavelengths where bandstructure calculations are problematic. Since the characteristics (e.g. angular pattern) of the third-harmonic light primarily depend on the fundamental mode dispersion, they could be readily engineered.

©2010 Optical Society of America

OCIS codes: (130.5296) Photonic crystal waveguides; (190.4390) Nonlinear optics, integrated optics; (190.4160) Nonlinear optics, multiharmonic generation.

References and links

1. T. Baba, "Slow light in photonic crystals," *Nat. Photonics* **2**(8), 465–473 (2008).
2. M. Soljacić, and J. D. Joannopoulos, "Enhancement of nonlinear effects using photonic crystals," *Nat. Mater.* **3**(4), 211–219 (2004).
3. N. A. R. Bhat, and J. E. Sipe, "Optical pulse propagation in nonlinear photonic crystals," *Phys. Rev. E Stat. Nonlin. Soft Matter Phys.* **64**(5), 056604 (2001).
4. J. F. McMillan, X. D. Yang, N. C. Panoiu, R. M. Osgood, and C. W. Wong, "Enhanced stimulated Raman scattering in slow-light photonic crystal waveguides," *Opt. Lett.* **31**(9), 1235–1237 (2006).
5. M. Ebnali-Heidari, C. Monat, C. Grillet, and M. K. Moravvej-Farshi, "A proposal for enhancing four-wave mixing in slow light engineered photonic crystal waveguides and its application to optical regeneration," *Opt. Express* **17**(20), 18340–18353 (2009).
6. C. Monat, B. Corcoran, M. Ebnali-Heidari, C. Grillet, B. J. Eggleton, T. P. White, L. O'Faolain, and T. F. Krauss, "Slow light enhancement of nonlinear effects in silicon engineered photonic crystal waveguides," *Opt. Express* **17**(4), 2944–2953 (2009).
7. Y. Hamachi, S. Kubo, and T. Baba, "Slow light with low dispersion and nonlinear enhancement in a lattice-shifted photonic crystal waveguide," *Opt. Lett.* **34**(7), 1072–1074 (2009).
8. A. Baron, A. Rysanyanskiy, N. Dubreuil, P. Delaye, Q. Vy Tran, S. Combrié, A. de Rossi, R. Frey, and G. Roosen, "Light localization induced enhancement of third order nonlinearities in a GaAs photonic crystal waveguide," *Opt. Express* **17**(2), 552–557 (2009).
9. K. Inoue, H. Oda, N. Ikeda, and K. Asakawa, "Enhanced third-order nonlinear effects in slow-light photonic-crystal slab waveguides of line-defect," *Opt. Express* **17**(9), 7206–7216 (2009).
10. C. Husko, S. Combrié, Q. V. Tran, F. Raineri, C. W. Wong, and A. De Rossi, "Non-trivial scaling of self-phase modulation and three-photon absorption in III-V photonic crystal waveguides," *Opt. Express* **17**(25), 22442–22451 (2009).
11. C. Monat, B. Corcoran, D. Pudo, M. Ebnali-Heidari, C. Grillet, M. D. Pelusi, D. J. Moss, B. J. Eggleton, T. P. White, L. O'Faolain, and T. F. Krauss, "Slow light enhanced nonlinear optics in silicon photonic crystal waveguides," *J. Sel. Top. Quantum Electron* **16**, 344–356 (2010).
12. H. Oda, K. Inoue, Y. Tanaka, N. Ikeda, Y. Sugimoto, H. Ishikawa, and K. Asakawa, "Self-phase modulation in photonic-crystal-slab line-defect waveguides," *Appl. Phys. Lett.* **90**(23), 231102 (2007).

13. B. Corcoran, C. Monat, C. Grillet, D. J. Moss, B. J. Eggleton, T. P. White, L. O'Faolain, and T. F. Krauss, "Green light emission in silicon through slow-light enhanced third-harmonic generation in photonic-crystal waveguides," *Nat. Photonics* **3**(4), 206–210 (2009).
14. L. O'Faolain, X. Yuan, D. McIntyre, S. Thoms, H. Chong, R. M. De la Rue, and T. F. Krauss, "Low-loss propagation in photonic crystal waveguides," *Electron. Lett.* **42**(25), 1454–1455 (2006).
15. J. Li, T. P. White, L. O'Faolain, A. Gomez-Iglesias, and T. F. Krauss, "Systematic design of flat band slow light in photonic crystal waveguides," *Opt. Express* **16**(9), 6227–6232 (2008).
16. A. Gomez-Iglesias, D. O'Brien, L. O'Faolain, A. Miller, and T. F. Krauss, "Direct measurement of the group index of photonic crystal waveguides via Fourier transform spectral interferometry," *Appl. Phys. Lett.* **90**(26), 261107 (2007).
17. X. Letartre, C. Seassal, C. Grillet, P. Rojo-Romeo, P. Viktorovitch, M. L. d'Yerville, D. Cassagne, and C. Jouanin, "Group velocity and propagation losses measurement in a single-line photonic-crystal waveguide on InP membranes," *Appl. Phys. Lett.* **79**(15), 2312–2314 (2001).
18. M. Notomi, K. Yamada, A. Shinya, J. Takahashi, C. Takahashi, and I. Yokohama, "Extremely large group-velocity dispersion of line-defect waveguides in photonic crystal slabs," *Phys. Rev. Lett.* **87**(25), 253902 (2001).
19. C. Comaschi, G. Vecchi, A. M. Malvezzi, M. Patrini, G. Guizzetti, M. Liscidini, L. C. Andreani, D. Peyrade, and Y. Chen, "Enhanced third harmonic reflection and diffraction in Silicon on Insulator photonic waveguides," *Appl. Phys. B* **81**(2-3), 305–311 (2005).
20. P. P. Markowicz, H. Tiriyaki, H. Pudavar, P. N. Prasad, N. N. Lepeshkin, and R. W. Boyd, "Dramatic enhancement of third-harmonic generation in three-dimensional photonic crystals," *Phys. Rev. Lett.* **92**(8), 083903 (2004).
21. N. Le Thomas, R. Houdre, L. H. Frandsen, J. Fage-Pedersen, A. V. Lavrinenko, and P. I. Borel, "Grating-assisted superresolution of slow waves in Fourier space," *Phys. Rev. B* **76**(3), 035103 (2007).
22. N. Le Thomas, R. Houdre, M. V. Kotlyar, D. O'Brien, and T. E. Krauss, "Exploring light propagating in photonic crystals with Fourier optics," *J. Opt. Soc. Am. B* **24**(12), 2964–2971 (2007).
23. S. G. Johnson, S. Fan, P. R. Villeneuve, J. D. Joannopoulos, and L. A. Kolodziejski, "Guided modes in photonic crystal slabs," *Phys. Rev. B* **60**(8), 5751–5758 (1999).
24. Y. Desieres, T. Benyattou, R. Orobchouk, A. Morand, P. Benech, C. Grillet, C. Seassal, X. Letartre, P. Rojo-Romeo, and P. Viktorovitch, "Propagation losses of the fundamental mode in a single line-defect photonic crystal waveguide on an InP membrane," *J. Appl. Phys.* **92**(5), 2227 (2002).
25. A. R. Cowan, and J. F. Young, "Mode matching for second-harmonic generation in photonic crystal waveguides," *Phys. Rev. B* **65**(8), 085106 (2002).
26. A. R. Cowan, and J. F. Young, "Nonlinear optics in high refractive index contrast periodic structures," *Semicond. Sci. Technol.* **20**(9), R41–R56 (2005).
27. D. Coquillat, J. Torres, D. Peyrade, R. Legros, J. P. Lascaray, M. Le Vassor d'Yerville, E. Centeno, D. Cassagne, J. P. Albert, Y. Chen, and R. M. De La Rue, "Equipfrequency surfaces in a two-dimensional GaN-based photonic crystal," *Opt. Express* **12**(6), 1097–1108 (2004).
28. J. Torres, D. Coquillat, R. Legros, J. P. Lascaray, F. Teppe, D. Scalbert, D. Peyrade, Y. Chen, O. Briot, M. L. d'Yerville, E. Centeno, D. Cassagne, and J. P. Albert, "Giant second-harmonic generation in a one-dimensional GaN photonic crystal," *Phys. Rev. B* **69**(8), 085105 (2004).
29. M. Centini, C. Sibilìa, M. Scalora, G. D'Aguanno, M. Bertolotti, M. J. Bloemer, C. M. Bowden, and I. Nefedov, "Dispersive properties of finite, one-dimensional photonic band gap structures: applications to nonlinear quadratic interactions," *Phys. Rev. E Stat. Phys. Plasmas Fluids Relat. Interdiscip. Topics* **60**(4 Pt B), 4891–4898 (1999).
30. Y. Dumeige, P. Vidakovic, S. Sauvage, I. Sagnes, J. A. Levenson, C. Sibilìa, M. Centini, G. D'Aguanno, and M. Scalora, "Enhancement of second-harmonic generation in a one-dimensional semiconductor photonic band gap," *Appl. Phys. Lett.* **78**(20), 3021–3023 (2001).
31. J. P. Mondia, H. M. van Driel, W. Jiang, A. R. Cowan, and J. F. Young, "Enhanced second-harmonic generation from planar photonic crystals," *Opt. Lett.* **28**(24), 2500–2502 (2003).
32. D. Coquillat, G. Vecchi, C. Comaschi, A. M. Malvezzi, J. Torres, and M. L. d'Yerville, "Enhanced second- and third-harmonic generation and induced photoluminescence in a two-dimensional GaN photonic crystal," *Appl. Phys. Lett.* **87**(10), 101106 (2005).
33. G. Vecchi, J. Torres, D. Coquillat, M. L. d'Yerville, and A. M. Malvezzi, "Enhancement of visible second-harmonic generation in epitaxial GaN-based two-dimensional photonic crystal structures," *Appl. Phys. Lett.* **84**(8), 1245–1247 (2004).
34. B. Corcoran, C. Monat, M. Pelusi, C. Grillet, T. P. White, L. O'Faolain, T. F. Krauss, B. J. Eggleton, D. J. Moss, "Optical performance monitoring via slow light enhanced third harmonic generation in silicon photonic crystal waveguides," *IEEE / OSA OFC, Postdeadline paper PDP A5* (2009)
35. B. Corcoran, C. Monat, M. Pelusi, C. Grillet, T. P. White, L. O'Faolain, T. F. Krauss, B. J. Eggleton and D. J. Moss, "Optical signal processing on a silicon chip at 640Gb/s using slow-light," submitted.

1. Introduction

Slow light propagation in photonic crystal (PhC) waveguides has attracted significant attention for its potential to increase the efficiency of nonlinear optical phenomena over short path lengths [1,2]. Following theoretical work that predicted such enhancement [2–5], several experimental demonstrations have confirmed this effect in the context of self-phase

modulation [6–9], interaction with free carriers [6,8], two- [6–9] and three- [10] photon absorption in both III-V semiconductors [8–10] and silicon [6,7]. These results demonstrate that slow light modes in PhC waveguides can induce nonlinear effects at lower input powers and in shorter waveguides [11] than fast light modes [12]. In addition, the wide bandwidth associated with some of these slow light features [6,7,11] should allow nonlinear optical signal processing on a chip at ultra-fast data rates.

Slow light propagation in PhC waveguides has also been shown to produce efficient third-harmonic generation (THG) [13] (another $\chi^{(3)}$ based nonlinear process), which manifests as the out-of-plane emission of (green) visible light from the conversion of a near-infrared optical pump coupled into the waveguide (see Fig. 1). In this context, the slow light PhC waveguide had two critical functions: (i) increasing the otherwise poor efficiency of the THG process, and (ii) allowing for the extraction of third harmonic (TH) visible light, before it was fully absorbed by silicon. In that work, we showed that slow light played a key role in determining the THG efficiency, estimated to be $\approx 10^{-7}$ for 10W coupled peak power.

This paper gives new insights into the underlying physics of THG in silicon PhC waveguides by investigating the role of phase matching between the fundamental mode and the TH light. The physics of this process is hard to determine theoretically, in part due to the difficulty of calculating reliable PhC bandstructures for silicon at visible wavelengths, in the presence of strong material dispersion and absorption. Here, by using Fourier optics, we directly measure the wavevector (equivalent to the outgoing angle of emission, see Fig. 1) of the TH light generated in slow light silicon PhC waveguides. We show that when tuning the wavelength of the near-infrared pump over $\sim 15\text{nm}$ in the slow light region, the TH light wavevector follows a variation imposed by the fundamental mode dispersion. This suggests that quasi-phase matching primarily dictates the characteristics of the TH light in these structures. We interpret these results as the coupling of the TH light to the continuum of radiation modes above the light line, which provides a relatively efficient pathway for THG in a system where the quasi-guided modes are (i) poorly matched with the fundamental mode, and (ii) have a finite lifetime, lowered by the absorption of silicon in the visible.

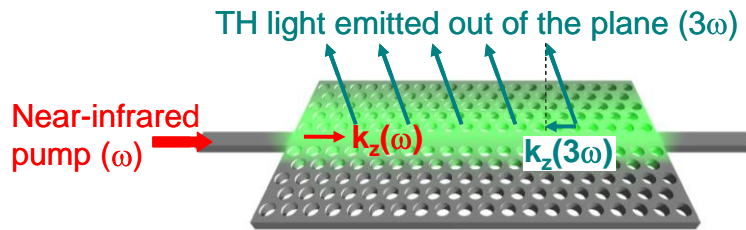


Fig. 1. Schematic of our experiment of THG in a PhC waveguide. The near-infrared pump signal (frequency ω , wavevector $k_z(\omega)$) is butt-coupled into the waveguide, while the TH light (3ω , $k_z(3\omega)$) is generated with an outgoing angle of emission that is directly related to the TH wavevector $k_z(3\omega)$.

2. THG induced green light emission in slow light silicon PhC waveguides

The silicon PhC waveguides are created within a periodic lattice of air holes (period $a = 410\text{nm}$) similarly to [6] and their fabrication is detailed in [14]; they are $80\mu\text{m}$ long, suspended in air, and connected to access ridge waveguides that are tapered in width close to the PhC waveguide (see inset of Fig. 2a) to improve light insertion from a butt-coupling arrangement of lensed fibers. The PhC waveguides are modified versions of the conventional W1 PhC waveguide created by omitting a single row of holes. Broadband slow light is obtained by slightly shifting the first two rows of holes either side of the waveguide core to engineer the fundamental mode dispersion [15], an example of which is displayed on Fig. 2a. The measured [16] spectral variation of group index n_g is represented on Fig. 2b and displays a typical “flat band” slow light window (grey area), where the group velocity is almost constant. Unlike other more common approaches that have been used to generate slow light

with a rapidly varying quadratic dispersion near the band-edge [8–10,17,18], this allows us to independently investigate the effect of phase matching and group velocity on THG efficiency.

We observe the out-of-plane THG visible light emission by butt-coupling TE polarised near-infrared optical pulses (4MHz, 8ps) from an amplified and filtered mode-locked fiber laser into the silicon PhC waveguide. Figure 2b shows the green light power when the pump wavelength is tuned between 1548nm and 1558nm, for a fixed pump power (≈ 10 W peak) coupled to the PhC waveguide having the dispersion of Figs. 2a, 2b. As already demonstrated in Ref [13] there is a strong correlation between the THG efficiency and the group velocity of the near-infrared pump signal. This dependence is even more striking here when probing the waveguide in the “flat band” slow light region (denoted as the grey area) where the group velocity does not vary significantly (see Fig. 2b), but the wavevector of the pump does (see Fig. 2a). The fact that the TH power is almost constant in this spectral window emphasizes the slow light dependence of THG, and the apparent negligible role of phase matching in this case, in agreement with the results reported in Ref [13].

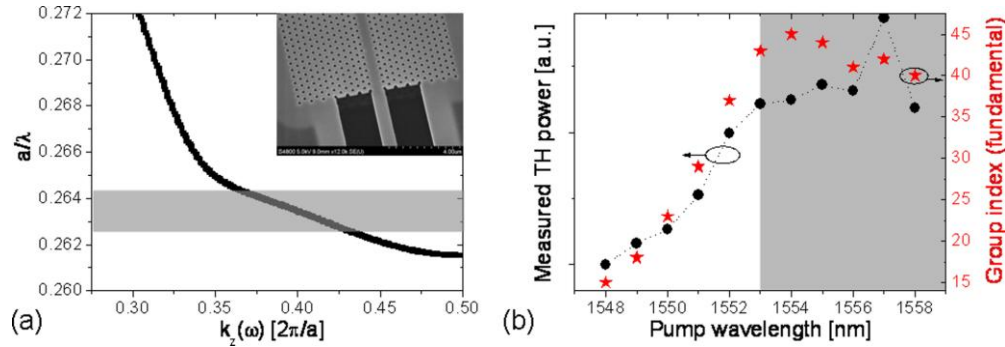


Fig. 2. (a) Calculated dispersion of the fundamental mode of a slow light engineered silicon PhC waveguide (inset: SEM image). (b) Average TH power (black circles) when tuning the wavelength of the pump with a fixed power, and measured group index (red stars) dispersion of the fundamental mode. The grey area denotes the spectral region where v_g is almost constant and equal to $\sim c/40$.

3. Measuring the wavevector dispersion of the THG induced green light

3.1 Phase matching and THG

The efficiency of THG in a homogeneous medium depends on phase matching between the fundamental beam (angular frequency ω , wavevector $k_z(\omega)$ along the propagation direction) and the TH beam (angular frequency $\omega_{TH} = 3\omega$, wavevector $k_z(\omega_{TH})$) as they co-propagate along the z direction. The conversion efficiency is maximum when those beams are perfectly phase matched, that is $k_z(\omega_{TH}) = 3k_z(\omega)$. The PhC partially relaxes this constraint: the THG efficiency is then maximum when $k_z(\omega_{TH}) = 3k_z(\omega) \pm mG$ (so-called quasi-phase matching [19]) with m being an integer, and G a reciprocal lattice vector of the PhC, here equal to $2\pi/a$.

In Ref [13], we demonstrated experimentally that the variation in THG efficiency with wavelength was consistent with slow light enhancement. We argued that the strong absorption of the TH light strongly weakened any effects of phase matching since the absorption length ($\sim 1\mu\text{m}$) at 3ω was much less than the coherence length ($\geq 2\mu\text{m}$) associated with the maximum phase mismatch between the fundamental and TH beams in the PhC waveguide. Here, we experimentally corroborate this argument by investigating this process more thoroughly. We systematically measure the TH wavevector $k_z(\omega_{TH})$ of the directive TH light emitted out-of-plane, in order to directly determine the role of phase matching between the two signals.

3.2 Imaging the third-harmonic light using Fourier optics

Because end-fire butt-coupling imposes a fixed position of the sample between the two lensed fibers, the angle of the green light emission cannot be directly measured through moving the

sample axis, as is done when probing harmonic generation in periodic structures using surface probe experiments [19,20]. Instead, we use a method inspired by the Fourier space imaging developed by Le Thomas et al. for retrieving the dispersion of PhC waveguide modes in the near infra-red [21,22]. The idea is to directly measure the wavevector of the green light emitted out of the chip through a suitable combination of lenses, as schematically represented in Fig. 3. In this way we image, onto the CCD2, the sample in the Fourier plane at the TH frequency ($\sim 520\text{nm}$), while observing the real image of the waveguide on the CCD1.

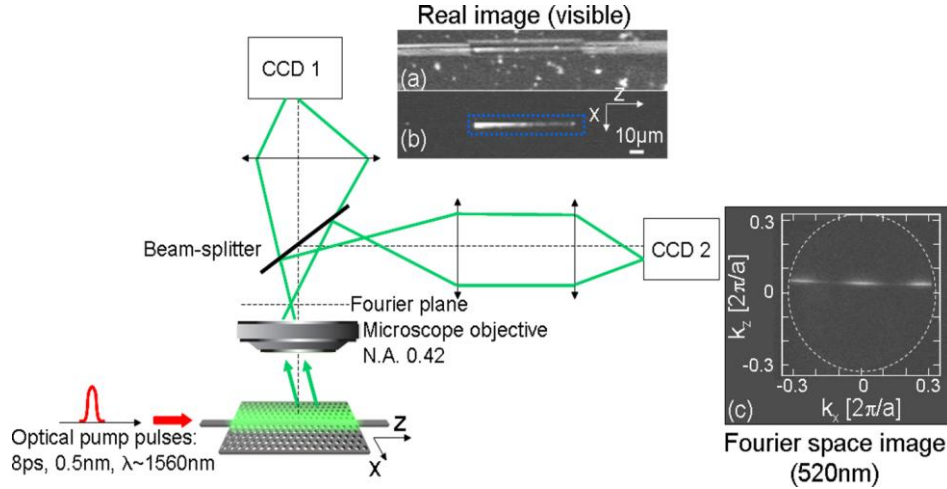


Fig. 3. Set-up used to measure the angle, and in turn, the wavevector of the TH light, generated out of the plane from the conversion of a near-infrared pump signal butt-coupled into the silicon PhC waveguide. A real image of the sample is produced onto CCD1 (inset a,b), while the associated image in the Fourier space (i.e. k -space) is produced onto the CCD2 at $\sim 520\text{nm}$ (inset c).

The images onto CCD1 (Figs. 3a, 3b) show the spatial pattern of the green light emission along the waveguide axis: the strong decay observed in the direction of propagation is mostly due to the linear and nonlinear absorption of the fundamental mode, as enhanced by slow light [11,13]. The images onto CCD 2 (see Fig. 3c) typically display one or several narrow lines that are elongated in the direction perpendicular to the waveguide axis z due to the optical confinement across the waveguide width. The position of these lines along the z direction is related to the outgoing angle of the generated TH light, from which we infer the wavevector component $k_z(\omega_{\text{TH}})$ of the TH mode supported by the PhC waveguide above the light line.

3.3 Results: dispersion of the third-harmonic generated light

We measure the dependence of $k_z(\omega_{\text{TH}})$ while tuning the wavelength of the near-infrared pump (between 1542nm and 1558nm). Detectable green light emission was observed throughout this wide spectral range due to the relatively high THG efficiency provided by the low group velocity (between $\sim c/15$ and $c/50$) of the fundamental mode over this 15nm spectral window. Figure 4a shows some of the collected Fourier space images and Fig. 4b displays on a 2D map the inferred dispersion ($k_z(\omega_{\text{TH}}), \omega_{\text{TH}}$) of the THG induced light. While knowledge of the absolute value of the $k_z(\omega_{\text{TH}})$ wavevector would require an accurate calibration step, we obtain a reliable measurement of the relative dispersion $k_z(\omega_{\text{TH}})$ expressed in the standard units of $[2\pi/a]$ by using the diameter of the objective N.A. ($= 0.42$) limitation visible onto the CCD2 images (white dashed circle on Fig. 3c).

From the bandstructure calculations (using a 3D plane wave expansion method) of the fundamental mode, we also plot on Fig. 4b, the dispersion curve ($k_z(3\omega), 3\omega$) corresponding to the case where quasi-phase matching would be met, that is $k_z(3\omega) = 3k_z(\omega) - 2\pi/a$. This red line curve corresponds to a 3 times stretched replica of the fundamental mode dispersion ($k_z(\omega), \omega$) folded back into the 1st Brillouin zone. The dispersion of the brightest feature of the 2D map

of Fig. 4b follows surprisingly well the dispersion calculated from the quasi-phase matching condition. Despite a horizontal and constant Δk_z shift, the relative $k_z(3\omega)$ experimental dispersion almost coincides with the stretched dispersion of the fundamental mode. This Δk_z shift ($\sim 0.03 [2\pi/a]$) corresponds to a 2 degrees offset deviation of the objective optical axis from the direction perpendicular to the chip.

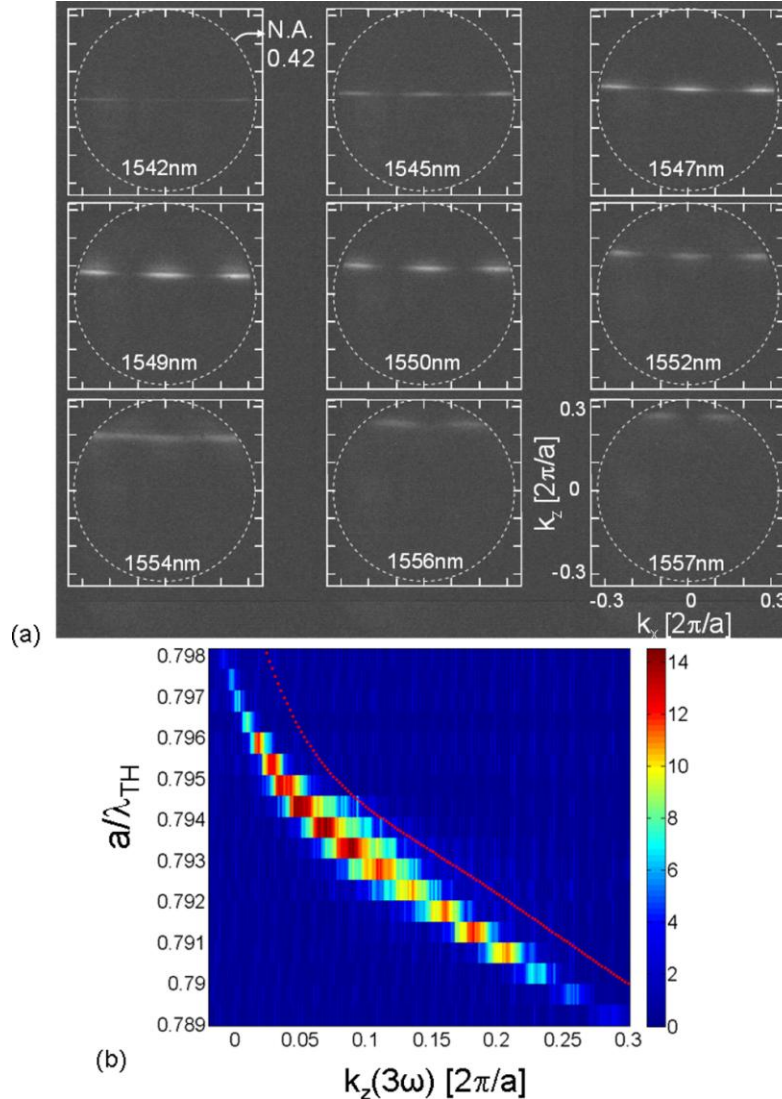


Fig. 4. (a) Fourier space images of the slow light silicon PhC waveguide W14816 at the TH frequency, when tuning the wavelength of the pump between 1542nm and 1557nm. (b) 2D map of the TH light dispersion ($k_z(\omega_{TH})$, $\omega_{TH} = 3\omega$) inferred from these images (colorbar increases with the green light intensity). The quasi-phase matching condition ($3k_z(\omega) - 2\pi/a$, 3ω) predicted from the calculated fundamental mode dispersion ($k_z(\omega)$, ω) is superimposed (red dots).

It is highly unlikely that one mode around the TH frequency has the required dispersion to exactly meet the quasi-phase matching condition over the 15nm spectral window, and approximate 2D calculations of the bandstructure around the TH frequency did not show any evidence of that [13]. Instead, these results suggest that the density of modes at the TH frequency is so large that there will always be at least one mode that can support the green light emission while ensuring quasi-phase matching with the fundamental. This interpretation

is reinforced by the change in the green light mode pattern in Fig. 4a when tuning the pump beam from 1547nm to 1557nm: the central antinode is progressively replaced by a node, which suggests that different modes support the TH emission at different pump wavelengths.

We probed two other slow light engineered PhC waveguides with slightly different dispersion and observed similar results. The $k_z(3\omega)$ wavevector associated with the brightest feature exhibited on the CCD2 images primarily follows the variation imposed by the quasi-phase matching condition with the fundamental (see Figs. 5a, 5b). In addition, when correcting for the systematic $\Delta k_z (= 0.03)$ offset common to all measured TH dispersions, we obtain, for the brightest features of the 2D maps of Figs. 4 and 5, three distinct spectral variations ($k_z(3\omega)$, 3ω) that are in very good agreement with the respective fundamental mode stretched dispersions (see Fig. 5c). This reemphasizes the primary dependence of the excited TH mode on the fundamental mode dispersion, which differs from guide to guide.

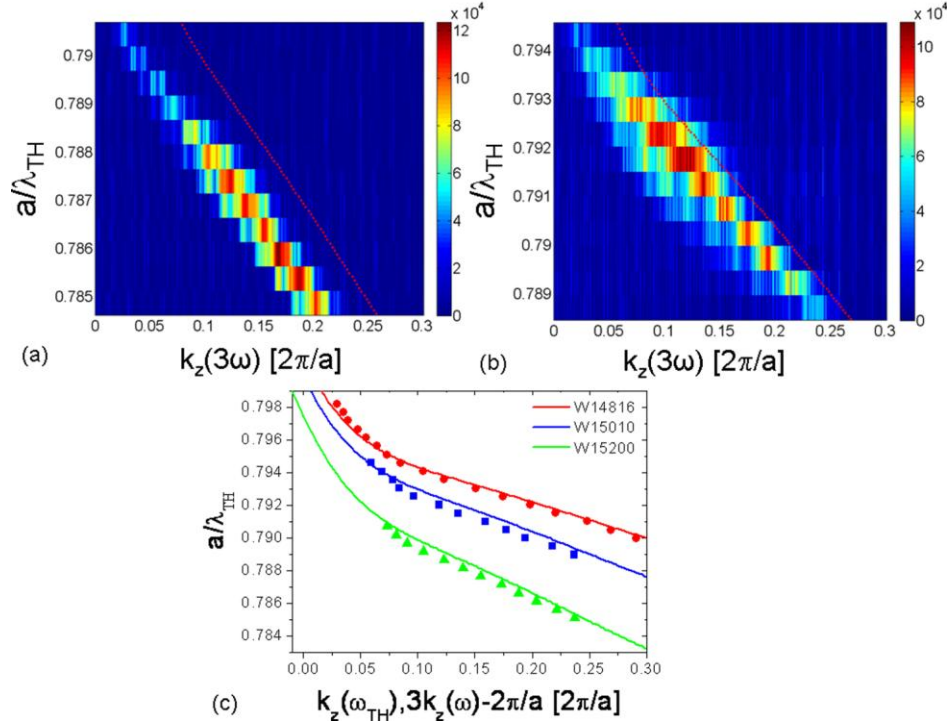


Fig. 5. (a,b) Dispersion ($k_z(\omega_{TH}), \omega_{TH} = 3\omega$) of the TH, inferred from the CCD2 images for two slow PhC waveguides ((a) W15200, (b) W15010) with different dispersion. (c) Comparison between the measured TH dispersion extracted from the brightest features of Fig. 4(b) and Figs. 5(a,b) (dots), and the quasi-phase matching condition ($3k_z(\omega) - 2\pi/a$, 3ω) predicted from the calculated fundamental mode dispersion ($k_z(\omega)$, ω) for each waveguide (solid lines). All experimental TH dispersion in (c) have been shifted by a constant $\Delta k_z = + 0.03 [2\pi/a]$ offset.

Concluding from these results that the modes at the TH frequency only consist of a continuum of states would not be accurate. For instance, the images displayed on Figs. 6a and 6b, which are associated with the waveguides of Figs. 5a, 5b excited at a particular pump wavelength, exhibit several discrete lines. We attribute these lines to distinct modes at the TH frequency which are all closely enough phase matched with the fundamental mode to be excited, thereby competing to support the TH field.

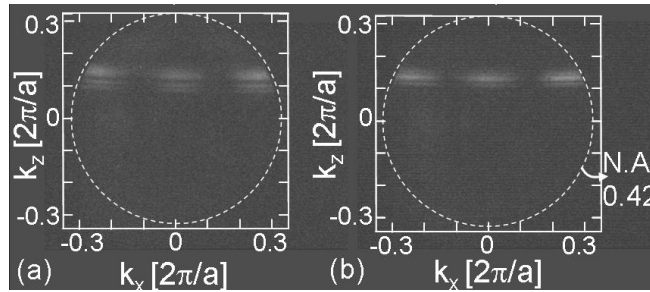


Fig. 6. (a,b) Fourier space images of the THG induced green light emitted from two different slow light PhC waveguides pumped at 1554nm.

4. Discussion

To discuss these results, it is worthwhile reviewing the classification of modes supported by PhC slabs. Leaving the linear defect aside, PhC slabs support three kinds of modes: (I) truly guided modes (like the one sustaining the pump signal) that are confined in the slab and propagate without any intrinsic loss, (II) quasi-guided (resonant) modes that are still bound to the slab but are intrinsically leaky, and (III) radiation (non resonant) modes that are not confined in the slab [23,24]. The in-plane wavevector of these modes lies either below (modes I) or above (modes II and III) the light line of the cladding material. While the dispersion of the Bloch modes of type I and II exhibit discrete bands, radiation modes III form a continuum above the light line.

Because the 1st Brillouin zone at the TH frequency lies entirely above the light line, THG in our structures converts the guided fundamental mode to either a quasi-guided mode II or a radiation mode III, both of which are, at least partially, coupled out of the plane. In practice, these resonant and non resonant modes provide competing channels for supporting the TH light, and the predominant pathway is determined by their relative conversion efficiencies [25,26]. Quasi-phase matching of the fundamental and the TH wavevectors is essential for high THG efficiency, even if the TH mode is not a truly propagating mode, in which case, a generalized residual version of the quasi-phase matching condition still prevails [25]. Due to the continuum of radiation modes III in the (k, ω) space, there is always a radiation mode for which quasi-phase matching is guaranteed. By contrast, quasi-phase matching with resonant modes II is only met when their dispersion coincides with the stretched dispersion of the fundamental mode [25–27]. This latter situation has been shown to produce local maxima in the conversion efficiency of second harmonic generation (SHG) within 1D and 2D periodic lattices, due to the field localization of the resonant modes in the nonlinear slab [25,28]. However, this phenomenon is not always observed in 2D periodic geometries because, unlike in (1D) Bragg periodic structures [28–30] mode matching is more complex than just matching the wavevectors of the fundamental and generated beams [26]. In addition, due to the leaky nature of the TH modes above the light line, the THG efficiency also depends on the (finite) lifetime of these modes, which is here strongly reduced by absorption.

The continuously phase matched character of the TH light measured in section 3 suggests that coupling the TH light to a (quasi-phase matched) radiation mode forms in our structures the preferential pathway for THG. Although evidence of quasi-guided modes is noticeable on some of the recorded images (Fig. 6), their presence does not seem to strongly influence the THG efficiency. Little improvement is apparently gained by coupling the TH to a resonant mode rather than to a non resonant mode. A similar effect was previously observed for SHG in planar PhCs, in which the doubly resonant conversion did not provide much additional enhancement over the resonant to non resonant conversion [31,26]. The absence of superimposed local enhancement when crossing the dispersion of resonant modes is here attributed to (i) the poor mode matching between the resonant modes at 3ω and the fundamental, and (ii) the low Q-factor or lifetime associated with these resonant modes, due to strong absorption of silicon at visible wavelengths.

In general, several parameters have been identified for increasing harmonic generation efficiency in periodic structures: (1) local field enhancement produced, for instance, by slow light, (2) coupling to (resonant or guided) modes localized into the slab, (3) fulfillment of the quasi-phase matching condition, and (4) the spatial overlap between the fundamental and harmonic modes, defining along with (3) a generalized “mode matching” condition, as relevant to 2D PhC geometries [26]. The quasi-phase matching condition is guaranteed by the coupling to radiation modes in the absence of resonant modes correctly matched with the fundamental. Arguments (1) and (2) (field localization, slowing down) are *a priori* desirable for both the fundamental and the TH light. Here, field localization is likely to be detrimental for the TH beam due to the strong material absorption at the TH frequency, whereas it is critical for the pump beam given the nonlinear dependence of the THG efficiency on the pump electric field intensity. In addition to slowing down of the fundamental to increase the THG efficiency through (1), the condition (2) is here naturally guaranteed for the fundamental by the butt-coupling configuration, which enables the excitation of an intrinsically lossless guided mode (I) that is strongly confined within the linear defect PhC waveguide. Note that all free-space coupling schemes used previously for probing SHG and THG were able to couple the fundamental to, at best, resonant modes with a finite lifetime [31–33]. The overall external conversion efficiency depends not only on the internal conversion efficiency between the incoming and outgoing modes, but also on the coupling efficiency of the outgoing mode to the upper half space, which is, here, a priori maximum for radiation modes.

While quasi-phase matching between resonant PhC modes is considered as a way to further increase the efficiency of SHG and THG processes, it generally occurs over narrow bandwidths. By contrast, we obtain here a relatively high THG efficiency whenever the group velocity of the pump is low enough, through the conversion of the guided fundamental mode into the continuum of radiation modes. This allows THG in our system to occur over a broader bandwidth, making it suitable for high-speed nonlinear operation. We have demonstrated, in particular, that the emission of green light was sensitive to signal impairment and thus could be used for monitoring the quality of near-infrared optical data at 160Gbit/s [34] and 640Gbit/s [35].

While calculations of a reliable bandstructure at the TH frequency have proved to be difficult due to the strong material dispersion and absorption, these results highlight that knowledge of the fundamental mode dispersion alone is sufficient to optimize, engineer and predict, to first approximation, the spectral and angular characteristics of the TH light emission. For instance, we could increase the collection efficiency of the green light by engineering the PhC waveguide, such that the quasi-phase matched TH has a close to vertical angle of emission. Another interesting consequence is that THG provides a nonlinear spectroscopic tool for probing the dispersion of the PhC waveguide fundamental mode itself with a simple (no interferometer) technique.

5. Conclusion

We have used Fourier optics techniques to measure the dispersion of THG induced visible light emission from slow light silicon PhC waveguides by directly probing the wavevector (equivalently, the outgoing angle) of the directive TH light emitted out-of-plane. The results reveal that the characteristics of the TH light are governed by the dispersion of the fundamental mode, via quasi-phase matching conditions. We infer that, in this geometry, THG involves the conversion of the well-confined and guided near-infrared fundamental mode into the continuum of radiation modes of the PhC slab above the light line at the TH frequency. The absence of any evident local maxima in the THG efficiency expected from coupling to resonant modes at 3ω is attributed to the low lifetime of these modes, which is greatly reduced by material absorption, and to their poor mode matching with the fundamental. The continuum of radiation modes form a reservoir of quasi phase matched modes at 3ω that supports THG with a reasonable efficiency, and most importantly over a substantial bandwidth, only limited by the group velocity of the pump. The fact that the characteristics (spectral, angular pattern) of the TH light primarily depend on the fundamental

mode of the PhC waveguide makes it possible to engineer and predict the TH properties, while, conversely, it gives information about the fundamental mode itself.

Acknowledgements

We acknowledge Nicolas Le Thomas for helpful discussions. The support of the Australian Research Council through its Centre of Excellence and Discovery Grant programs is gratefully acknowledged. Additional acknowledgment is given to the support of the Department of Education, Science and Technology through the International Science Linkages program. The silicon samples were fabricated in the framework of the EU-FP6 funded ePIXnet Nanostructuring Platform for Photonic Integration (www.nanophotonics.eu).